

## Chapter 5 Surface Waves

### Post-Critical Planar SH waves

In the last chapter we discussed how to solve the problem of a planar SH-wave incident from a half space onto the bottom of a layer welded on that half space. In this case, there were no post-critical angle reflections in the problem. However, there are instances in which plane waves can travel horizontally such that there is a critical reflection of the wave at the boundary between the layer and the half-space. In this case the waves are totally reflected at the top and the bottom of the layer and it becomes trapped within the layer. This problem is similar to the propagation of planar SH-waves in a plate that was also discussed in the last chapter. However, this problem differs in that the plate problem had traction free boundaries above and below, while the current problem has an elastic half-space below. In order to solve this problem, we must investigate the nature of critically reflected waves. Consider the problem of a planar harmonic SH-wave that is incident on the boundary of two welded spaces, as was shown in Figure 4.2 of the previous chapter. A general expression for such a wave can be written as

$$\mathbf{u}(\mathbf{x}, t) = A \mathbf{d} \exp[ik(\mathbf{x} \cdot \mathbf{p}) - ct] \quad (5.1)$$

where the motion is either the real or imaginary part of the right hand side of (5.1).  $A$  is a complex number whose modulus is the amplitude of the wave,  $\mathbf{d}$  is a unit vector in the direction of the particle motion,  $\mathbf{p}$  is a unit vector in the direction of propagation (perpendicular to the wavefront), and  $c$  is the phase velocity in the direction of  $\mathbf{p}$ .  $k$  is the wavenumber, and it is related to the wavelength  $\Lambda$ , period  $T$ , and angular frequency  $\omega$ , by

$$\omega = kc = \frac{2\pi}{T} \quad (5.2)$$

$$k = \frac{2\pi}{\Lambda} \quad (5.3)$$

Using this notation we can write the incident SH wave shown in Figure 5.1 as

$$u_2^I = A_I \exp[ik_I(x_1 \sin \theta_1 + x_3 \cos \theta_1 - \beta_1 t)] \quad (5.4)$$

The reflected wave is

$$u_2^R = A_R \exp[ik_I(x_1 \sin \theta_1 - x_3 \cos \theta_1 - \beta_1 t)] \quad (5.5)$$

and the transmitted wave is

$$u_2^T = A_T \exp[ik_T(x_1 \sin \theta_2 + x_3 \cos \theta_2 - \beta_2 t)] \quad (5.6)$$

If the reflection is post-critical, then  $\sin \theta_2 = (\beta_2/\beta_1) \sin \theta_1 > 1$ , and since  $\cos \theta_2 = \sqrt{1 - \sin^2 \theta_2}$ , then  $\cos \theta_2$  is imaginary. In this case, the transmitted wave (5.6) is given by

$$u_2^T = A_T \exp(-bx_3) \exp[ik_1(x_1 \sin \theta_2 - \beta_2 t)] \quad (5.7)$$

where

$$b = k_1 \sqrt{\left(\frac{\beta_2^2}{\beta_1^2}\right) \sin^2 \theta_1 - 1} \quad (5.8)$$

(5.7) means that the disturbance into the second medium dies exponentially with the distance from the interface, with longer wavelength harmonic waves disturbing regions further into the medium than do short wavelengths. The reflection coefficient  $A_R$  becomes complex with a modulus of 1 for post-critical reflections. That is,

$$A_R = \frac{\mu_1 \cos \theta_1 - \mu_2 \left(\frac{\beta_1}{\beta_2}\right) \cos \theta_2}{\mu_1 \cos \theta_1 + \mu_2 \left(\frac{\beta_1}{\beta_2}\right) \cos \theta_2} \quad (5.9)$$

When  $\cos \theta_2$  is imaginary (post-critical reflection), then the modulus of  $A_R$  is 1. The fact that  $A_R$  is complex means that a phase shift  $\delta$  is introduced in the reflected wave given by (5.5). This phase shift is a number that depends on the velocity contrast and the incidence angle, but it does not depend on the wavelength. This means that the location of the crests of the incident waves at the boundary are offset by a constant percentage of the wavelength from the crests of the reflected waves as is shown in Figure 5.1. In a sense, it almost looks as if the wave is reflected at some virtual point beneath the boundary, where the depth of the virtual bounce point increases with the wavelength of the wave.

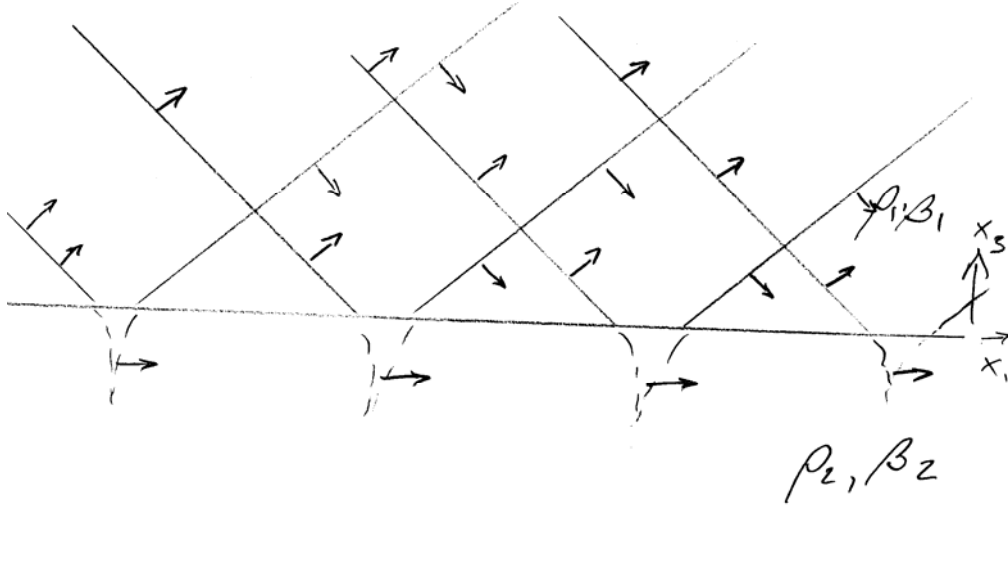


Figure 5.2 Critically reflected planar SH-waves.

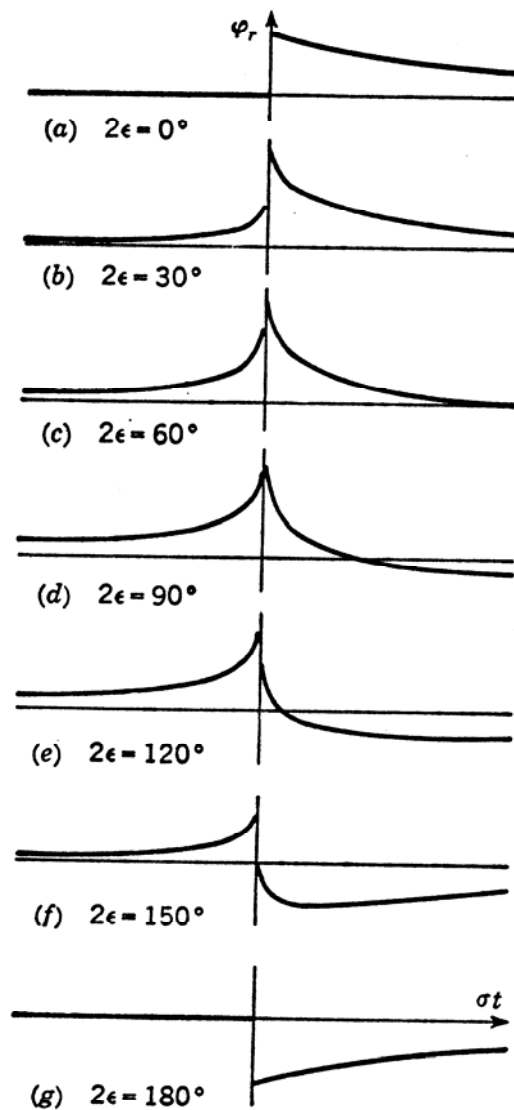


FIG. 3-17. Shape of reflected pulse for several values of phase change  $2\epsilon$ , computed from Eqs. 3-50. (After Arons and Yennie.)

Figure 5.3 This figure shows the effect of the phase lag introduced by the complex reflection coefficient on an incident wave that consists of a step in displacement. The reflected wave has a very different time behavior. At the time of the expected geometric reflection, the waveform locally looks like it is the time derivative of the incident wave.

While this constant phase shift is relatively easy to understand for a harmonic plane wave, things get more complex if we consider the case of an impulsive wave. Such waves can be considered to be the superposition of harmonic waves. However, the effect of phase-shifting the reflected harmonic waves can be rather dramatic. Figure 5.2 demonstrates the shape of the reflected wave for different phase lags; the top trace is the

shape of the incident wave. Notice the rather surprising fact that the reflected wave actually starts at minus infinite time (long before the incident wave begins its motion). This is a rather unusual consequence of the fact that we have assumed a planar incident wave. Such waves can never really exist in nature since they require infinite spaces with waves that travel throughout all time. Nevertheless, there is always a disturbance in the lower medium that precedes a critically reflected incident wave. This is the inevitable result of the fact that there is no wave in the slower medium that can travel as slowly as the phase velocity of the incident wave along the interface.

## Diffraction vs. Refraction

Waves that can be fully described by their ray paths (Snell's Law) are generally referred to as **refracted** waves; this is really the same thing as saying that the waves can be considered to be plane waves that are propagating through a plane layered medium without any critical angle reflections. In truth, nothing in the Earth actually does this, and in many cases wave propagation is very different from that of plane waves. Waves that **are not** refracted are called **diffracted**. In a sense, the phase lag introduced in a critically reflected wave is an example of diffraction.

## Love Waves

If we now consider the case of SH-plane waves propagating in a low-velocity layer over a half-space, we see that we have a situation that is very similar to the plate-wave problem of Chapter 4, except that we now have a critical reflection to deal with at the bottom of the layer. Although the wave is totally reflected at the bottom of the layer, there is a phase lag associated with the critical reflection. The wavefronts are sketched in Figure 5.3. The phase velocity dispersion relation is similar to that given in the last chapter for a plate, but an additional lag must be introduced to account for the phase shift of the critical reflection. Love waves can only occur if the surface layer has a lower velocity than the whole space.

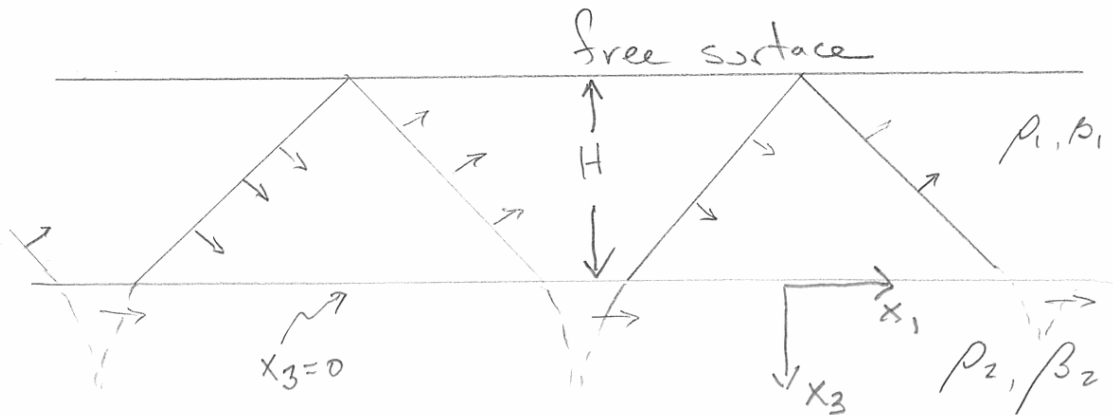


Figure 5.3. A love wave can be thought of as a plane wave that is trapped in a low velocity layer at the surface of the earth.

Love waves were actually observed on seismometers long before they were explained, by A.E.H. Love. Although it is possible to derive the solution as series of critically reflected SH waves, it is also possible to derive the solution to this problem by investigating solutions of the form given below. As it turns out, the solutions for a harmonic Love wave traveling in the  $x_1$  direction in a layer of thickness  $H$  overlying a half space as shown in Figure 5.3, are given by

$$u_2 = A_2 \exp \left[ -kx_3 \sqrt{1 - \frac{c^2}{\beta_2^2}} \right] \exp [ik(x_1 - ct)] \quad (5.10)$$

in medium 2 (i.e.,  $z > 0$ ), and

$$u_2 = \left\{ A_1 \exp \left[ -kx_3 \sqrt{1 - \frac{c^2}{\beta_1^2}} \right] + A'_1 \exp \left[ kx_3 \sqrt{1 - \frac{c^2}{\beta_1^2}} \right] \right\} \exp [ik(x_1 - ct)] \quad (5.11)$$

in medium 1 (the layer).  $u_1 = u_3 = 0$  everywhere in the medium. Unfortunately, these motions seem rather complex to just pick out of a hat. However, it can be shown that they do satisfy Navier's equation. If  $c < \beta_2$ , then we have a solution that dies exponentially in amplitude with distance below the interface. Now (5.10) and (5.11) are acceptable solutions to the geometry shown in Figure 5.3 if i) the motion  $u_2$  is continuous across the boundary at  $x_3 = 0$ , ii) the stress  $\sigma_{23}$  is continuous across the boundary  $x_3 = 0$ , iii) and the stress  $\sigma_{23} = 0$  on the free surface at  $x_3 = -H$ . By imposing these conditions on (5.10) and (5.11), we can find conditions on  $c, A_2, A_1$ , and  $A'_1$  which provide an acceptable solution. By following this procedure, one can show that for an acceptable solution, the phase velocity  $c$  depends not only on the intrinsic velocities  $\beta_1$  and  $\beta_2$ , but also on the frequency of the wave. That is, the wave is dispersive. It is also generally true that  $\beta_1 < c < \beta_2$ . Furthermore, low frequency Love waves tend to have phase velocities that approach those of the high-velocity half space, whereas short period love waves tend to have phase velocities close that of the low-velocity layer (at least that is true for the fundamental mode Love waves). As was the case for plate waves, there are also higher mode Love waves, but their derivation is more complex because of the critical reflection.

Love waves can be generated by a source located at a point (called a **point source**). In this case, Love waves are observed on the **transverse component** of motion. Since Love waves have their motions near the top of the elastic medium, their energy spreads as an expanding circle along the surface. That is the energy flux associated with Love waves must be conserved for any outward traveling wave. Since the circumference of a circle grows as  $r$ , and since energy depends on  $\dot{u}^2$ , the amplitude of Love waves must decay as  $\frac{1}{\sqrt{r}}$  for Love waves radiated by a point source. Thus, as the observer distance becomes larger, the Love waves become larger relative to other waves whose amplitude decays as  $\frac{1}{r}$ . It is generally true that at large distances, surface waves tend to be larger than body waves.

## Rayleigh Waves

The Rayleigh wave is a special solution to the equation of motion; it has the characteristic that it allows zero traction along a boundary. We will discuss the simplest example of a Rayleigh wave; that is, a two dimensional plane Rayleigh wave that propagates at velocity  $c$  in the  $x_1$  direction as is shown in Figure 5.4.

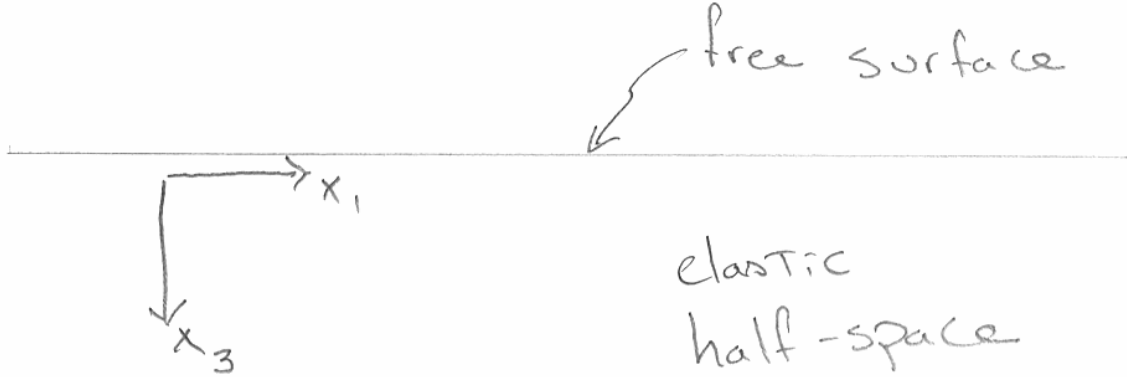


Figure 5.4

The material is an elastic half-space and the surface  $x_3 = 0$  is traction free, or

$\sigma_{13}|_{x_3=0} = \sigma_{23}|_{x_3=0} = \sigma_{33}|_{x_3=0} = 0$ . Consider the motion

$$u_1 = \Re \left\{ A \exp(-bx_3) \exp[ik(x_1 - ct)] \right\} \quad (5.12)$$

$$u_3 = \Re \left\{ B \exp(-bx_3) \exp[ik(x_1 - ct)] \right\} \quad (5.13)$$

$$u_2 = 0 \quad (5.14)$$

where  $b$  is a real constant,  $A$  and  $B$  are complex constants, and where  $\Re$  means to take the real part of the argument. Keep in mind that

$$\exp[ik(x - ct)] = \sin[k(x - ct)] + i \cos[k(x - ct)] \quad (5.15)$$

This solution represents a sine wave of wavelength  $\Lambda = 2\pi/k$ , which travels in the  $x_1$  direction with a velocity of  $c$ . For this to be a valid solution for our problem, we need to find the appropriate values of  $b$ ,  $A$ ,  $B$ , and  $c$ . Since we are only considering the real parts of the solution in (5.12) and (5.13), we have four unknowns and two boundary conditions at the free surface ( $\sigma_{23}|_{x_3=0} = 0$  is satisfied trivially because of (5.14)). Therefore

$$\sigma_{33}|_{x_3=0} = 0 = \lambda \left( \frac{\partial u_3}{\partial x_3} + \frac{\partial u_1}{\partial x_1} \right) + 2\mu \frac{\partial u_3}{\partial x_3} \quad (5.16)$$

and

$$\sigma_{13}|_{x_3=0} = 0 = \mu \left( \frac{\partial u_1}{\partial x_3} + \frac{\partial u_3}{\partial x_1} \right) \quad (5.17)$$

Furthermore, we must also satisfy Navier's equations, or

$$\rho \frac{\partial^2 u_1}{\partial t^2} = \mu \left( \frac{\partial^2 u_1}{\partial x_1^2} + \frac{\partial^2 u_1}{\partial x_3^2} \right) + (\lambda + \mu) \left( \frac{\partial^2 u_1}{\partial x_1^2} + \frac{\partial^2 u_3}{\partial x_1 \partial x_3} \right) \quad (5.18)$$

and

$$\rho \frac{\partial^2 u_3}{\partial t^2} = \mu \left( \frac{\partial^2 u_3}{\partial x_1^2} + \frac{\partial^2 u_3}{\partial x_3^2} \right) + (\lambda + \mu) \left( \frac{\partial^2 u_3}{\partial x_3^2} + \frac{\partial^2 u_1}{\partial x_1 \partial x_3} \right) \quad (5.19)$$

It is actually a rather laborious process to find the appropriate values of  $b$ ,  $A$ ,  $B$ , and  $c$  that satisfy these equations. However, the following solution does satisfy the conditions if the solid is considered to be Poissonian (i.e., Poisson's ratio =  $1/4$ , or  $\lambda = \mu$ ).

$$u_1 = D \left( e^{-0.8475 k x_3} - 0.5773 e^{-0.3933 k x_3} \right) \cos \left[ k (x_1 - c_R t) \right] \quad (5.20)$$

and

$$u_3 = D \left( -0.8475 e^{-0.8475 k x_3} + 1.4679 e^{-0.3933 k x_3} \right) \sin \left[ k (x_1 - c_R t) \right] \quad (5.21)$$

where

$$c_R = 0.9194 \sqrt{\frac{\mu}{\rho}} = 0.9194 \beta \quad (5.22)$$

Figure 5.5 shows a schematic of the particle motion for a harmonic Rayleigh wave in a half-space.

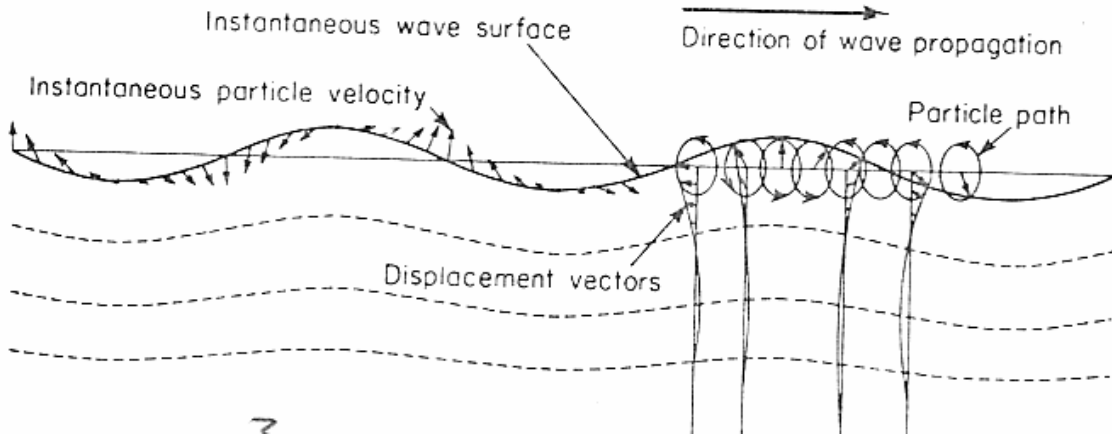


Figure 5.5 Snapshot in time of the particle motion for a harmonic Rayleigh wave in an elastic half-space.

Notice that the particle motion at the free surface is an ellipse for this harmonic wave. That is, the vertical component (which is about 150% larger in amplitude than the horizontal component) is a sinusoid and the horizontal component is a co-sinusoid (or the vertical and horizontal components are out of phase by  $\pi/2$ ). Notice also that, at the top

of the ellipse, the particle is moving in the opposite direction from the direction of the wave propagation. This is referred to as “retrograde particle motion,” and it is quite characteristic of Rayleigh wave. Also, notice that horizontal motions reverse their direction at a depth of about 0.192 times the wavelength  $\Lambda$  of the Rayleigh wave (or they have a node at this depth). That is, the horizontal motion is zero at  $0.192 \Lambda$  and the particle motion is prograde at larger depths.

Notice that Rayleigh wave velocities in a homogeneous half space are independent of the wavelength. That is, Rayleigh waves are non-dispersive in a homogeneous half-space. This is different from Love waves, which are inherently dispersive. However, Rayleigh waves are only non-dispersive in a homogeneous half-space. Shear wave velocities generally increase with depth in the Earth. Since long-wavelength Rayleigh waves have motions at a significantly greater depth than do short wavelength Rayleigh waves (remember they die as  $\exp(-z/\Lambda)$ ), the velocities of Rayleigh waves generally increases with wavelength for the Earth.

Just as was the case for Love waves, Rayleigh-wave energy generally spreads circularly from a point source and the amplitude of Rayleigh waves generally decrease as  $1/\sqrt{r}$  with distance from the point source. In the case of point sources, Rayleigh waves are generally observed on both the **radial and vertical** components of a seismographic station.

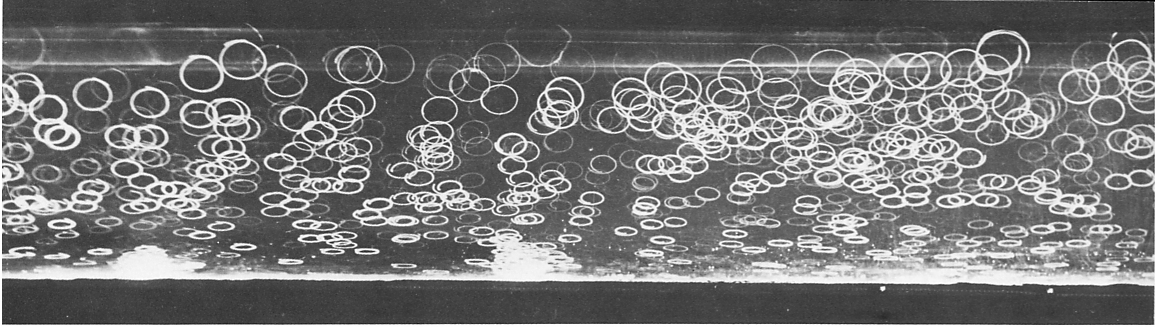
The solution demonstrated above is called a fundamental Rayleigh wave, and there are no nodes in the vertical motion as a function of depth (there is 1 node in the horizontal component with depth). The fundamental Rayleigh wave is the only surface wave that can occur in a homogeneous half-space. Love waves require at least one low velocity layer to be present. In addition to fundamental mode Rayleigh waves, there are solutions to the layered space that are similar to the Love wave case, but which involve P- and SV-waves. If the velocity of the upper layer is low enough so that both P- and SV-waves can be completely reflected (all reflections are post-critical), then there can be plate modes in the P-SV system just as there are in the SH system. These are referred to as **higher mode Rayleigh waves**. Just as with the Love wave case, they can be simplified into a harmonic wave with a horizontal phase velocity that is constant as a function of depth and also another function of depth (pseudo-harmonic) that describes the depth dependence of the mode. If some of the reflections (e.g. SV to SV) are post critical, but others are pre-critical (P to P), then there may be some wave energy that is continually radiated from the low-velocity layer. The system is no long a perfectly trapped system. These are referred to as **leaky modes**.

Excitation of fundamental mode Rayleigh waves is rather difficult to imagine. They cannot be generated by planar P- and S-waves incident on a planar free surface. As it turns out, the curvature of either a wavefront, or a free surface is critical to the generation of fundamental Rayleigh waves; the tighter the radius of curvature, the broader the frequency band of Rayleigh waves that can be generated. That means that deep earthquakes can only generate long-period fundamental Rayleigh waves, whereas shallow

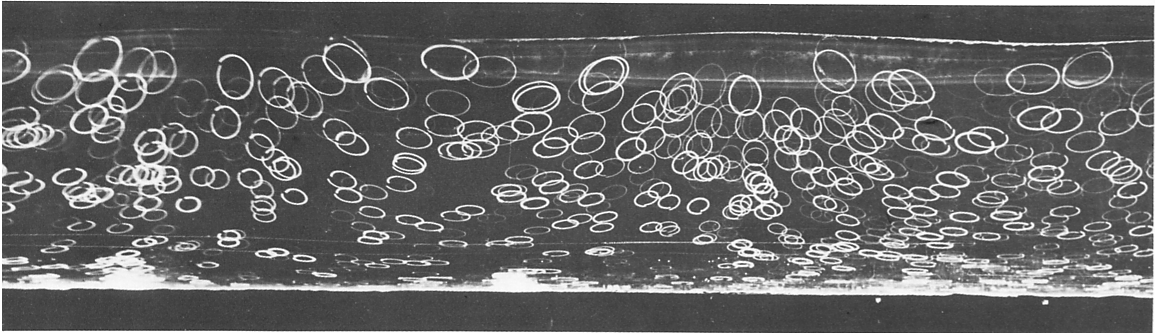


earthquakes generate broader-band surface waves. However, it is also true that fundamental P- and S-waves are much larger at high frequencies than Rayleigh waves.

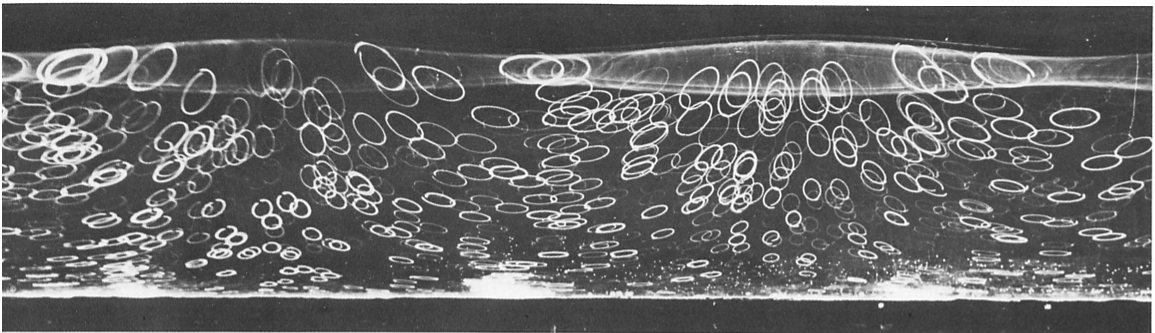
This fundamental Rayleigh wave has some mathematical similarities to the solution for gravity waves in the ocean (the type that make you sea sick). However, oceanic water waves have prograde particle motions as is shown in Figure 5.6. As is the case with any two identical wavetrains that are traveling in opposite directions, standing waves are formed. The series of figures show long exposures of gravity water waves traveling towards the right. The white streaks are white particle of neutral buoyancy. The ellipses are their particle motions. In each successive figure more left-traveling wave is added to the mix. In the final figure, one can see that there are purely standing waves. In this case the particle motions are no longer elliptical, but instead become purely linear. Notice that nodes for the horizontal motions are maxima for the vertical motions and vice versa.



No reflection: pure progressive waves



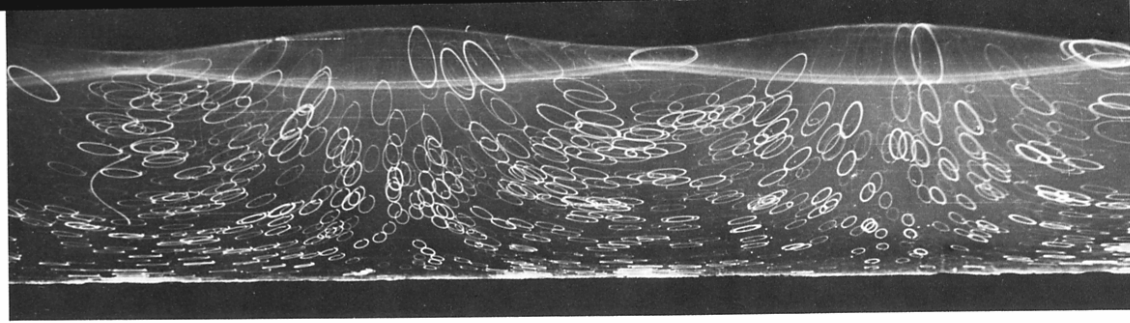
24% reflection



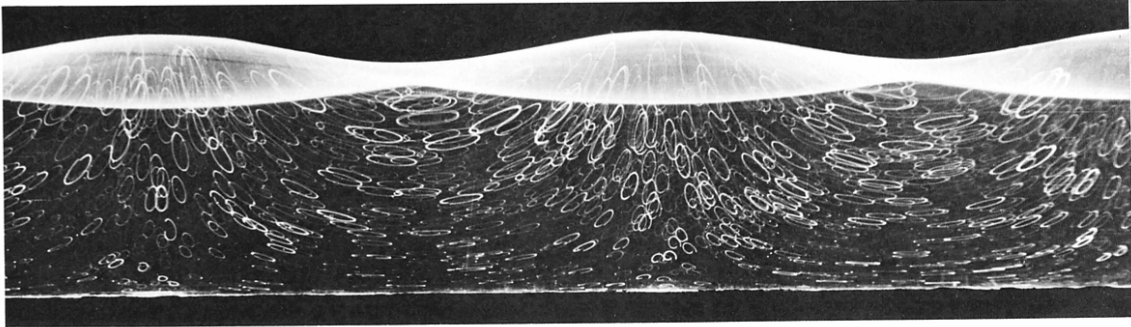
38% reflection

**191. Particle trajectories in plane periodic water waves.** Two wave trains of the same frequency traveling in opposite directions are produced by a progressive wave coming from the left that is reflected by a partially absorbent barrier. The top photograph shows the pure progressive wave with no reflection. Its amplitude is four per cent of the wavelength, and the water depth is 22 per cent. White particles suspended in the water are photographed during one period. Their trajectories are practically ellipses traversed clockwise, circular at the free surface and flat-

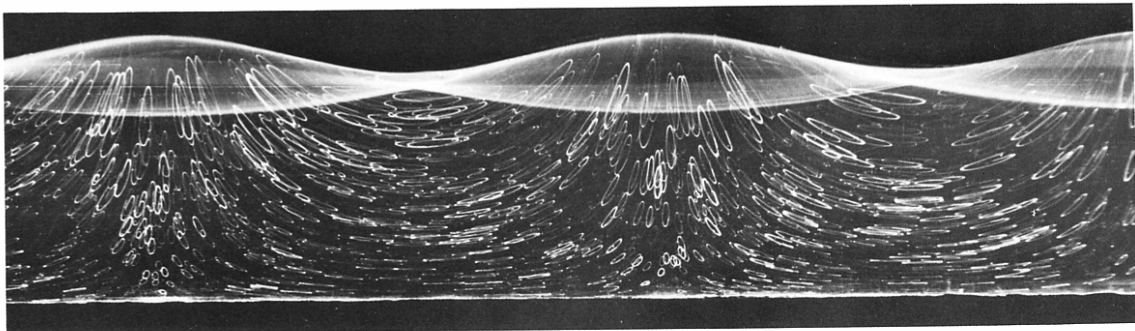
tened toward the bottom. Some open loops indicate a slow drift to the right near the surface and left near the bottom. As the reflection is increased, the orbits become increasingly flattened and inclined. Complete reflection gives a pure standing wave in the last photograph, where the trajectories are streamlines. There the upper and lower envelopes of the water surface show that the vertical motion does not vanish at the nodes. *Wallet & Ruellan 1950, courtesy of M. C. Vasseur*



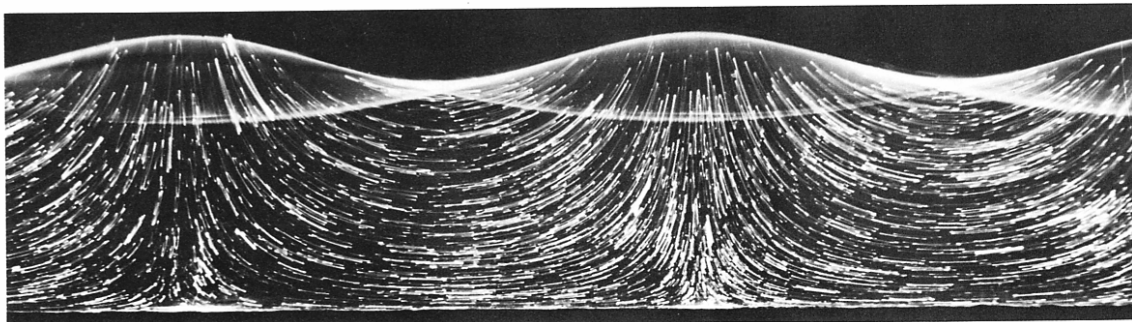
53% reflection



71% reflection



85% reflection



100% reflection: pure standing waves